

Detection and attribution of changes in 20th century land precipitation

F. Hugo Lambert

Department of Physics, University of Oxford, Oxford, UK

Peter A. Stott

Hadley Centre for Climate Prediction and Research, Met Office, Reading, UK

Myles R. Allen

Department of Physics, University of Oxford, Oxford, UK

Michael A. Palmer

Rutherford Appleton Laboratory, Didcot, Oxfordshire, UK

Received 21 January 2004; revised 2 April 2004; accepted 26 April 2004; published 20 May 2004.

[1] Observed globally-averaged land precipitation changes over the 20th century are compared with simulations of the HadCM3 climate model using an “optimal fingerprinting” method. We find that observed changes in precipitation are too large to be consistent with model-generated internal variability and are consistent with (attributable to) the combination of natural and anthropogenic forcings applied to the model. By comparing precipitation observations to shortwave and longwave forcing timeseries, we find that most of the forced variation in precipitation appears to be driven by natural shortwave forcings. We are unable to detect a response to anthropogenic longwave forcings in isolation. Finally, we seek to explain these results in terms of perturbations to the energy budget of the troposphere. *INDEX TERMS*: 1620 Global Change: Climate dynamics (3309); 1655 Global Change: Water cycles (1836); 3354 Meteorology and Atmospheric Dynamics: Precipitation (1854). **Citation**: Lambert, F. H., P. A. Stott, M. R. Allen, and M. A. Palmer (2004), Detection and attribution of changes in 20th century land precipitation, *Geophys. Res. Lett.*, 31, L10203, doi:10.1029/2004GL019545.

1. Introduction

[2] Optimal detection techniques, as described by *Allen and Stott* [2003], have been applied to compare observed and model simulated responses to changes in external factors forcing climate for a variety of climatic variables. *Stott et al.* [2000] and *Tett et al.* [2002] attributed changes in twentieth century large-scale near-surface temperature to a combination of natural and anthropogenic factors. Using a similar method, *Gillett et al.* [2003] established that observed changes in sea level pressure cannot be explained by internal climate variability alone.

[3] We expect changes in precipitation to be harder to attribute to external forcing because of difficulties with measuring and simulating precipitation and a lower signal to noise ratio. Accurate surface-based observations are only available since 1900 and are restricted to the Earth’s land-surface. Satellite datasets with global coverage do exist but none stretches back further than 1979 [e.g., *Spencer*, 1993], providing an insufficiently long dataset for us to explore the

historical dependence of precipitation on external forcing over decadal timescales. Therefore, we use a land-based dataset for the period 1900–98 [*Hulme*, 1992; *New et al.*, 2000] and neglect model data for which there are no corresponding observations.

2. Quantitative Comparison of Model Simulations and Observed Data

[4] A standard least squares “optimal fingerprinting” method [e.g., *Hasselmann*, 1993; *Allen and Stott*, 2003] is applied to the comparison of the observed data and a four-member ensemble of the coupled HadCM3 model [*Gordon et al.*, 2000]. The “ALL” ensemble is driven with anthropogenic greenhouse gas (GHG) and sulphate aerosols, and changes in solar output and volcanic aerosols [*Stott et al.*, 2000; *Johns et al.*, 2003]. An estimate of the indirect effects of aerosol particles on cloud optical properties was included in these simulations but no representation of black carbon [*Tett et al.*, 2002]. Two further ensembles are available: one driven with natural forcings alone, and one driven with anthropogenic forcings alone. However, it is not possible to detect the influence of external forcings in the observations with these runs, apparently because of a weak signal to noise ratio.

[5] It is assumed that the observations can be represented as a linear superposition of the model simulated responses to external forcings scaled by unknown amplitudes, β_i , and that both model and observed data are contaminated with climate “noise”. Four ensemble members are averaged together to increase the signal to noise ratio. The observations are expressed as globally-averaged anomalies about the mean climatology derived for the period 1961–90. In a given year, we include grid box data for which at least 7 of 12 months are present, although the results are insensitive to the selection criterion (see Figure 1a of *Hulme et al.* [1998] for a summary of the available observations). Model output is prepared identically to the observations, including “masking” out missing data. Model and observed data are projected onto principal components (PCs) of the model control run and weighted such that components containing the least internal variability are given most weight. Total least squares regression (TLS) is employed to estimate the values of β_i , allowing us to calculate the magnitude of the model-derived patterns required to best represent the real

world. $\beta > 1$ implies the model underestimates the response of the real world, and $\beta < 1$ implies the model overestimates it. The noise terms calculated from the TLS residual are compared with natural internal variability estimated from a control run of the HadCM3 model via an F -test where the noise is assumed to be multivariate normal. If the confidence limits enclosing the best estimate of β_i are entirely positive, the i th signal is said to be detected.

[6] We are focusing on global mean, 6-year averaged data, so we use all available PCs without further truncation, unlike studies investigating stronger forced signals and longer vectors [e.g., Gillett *et al.*, 2003; Allen and Stott, 2003].

3. Detection of External Influence on Land Precipitation

[7] First we show that the combined response to external forcing can be detected during the period 1944–97 by comparing observations with the ALL ensemble. Each observed and forced model ensemble mean was prepared as nine 6-year means beginning at 1944 and averaged over spatial grid points. β is estimated to be 2.22 with 5–95% confidence limits spanning 1.00 to 5.34 indicating that the model may be underestimating the response, also suggested by visual inspection of Figure 1a. The residual F -test P -value is 0.18, meaning that the remaining variance is consistent with model generated internal variability and suggesting that the forcings included in the model are sufficient to explain changes in observed precipitation. Hence the HadCM3 model appears to capture the form of the observed global precipitation behavior despite the problems noted in section 1.

[8] The influence of external forcings as simulated by the ALL ensemble is also detected for the period 1908–1997 but at a lower (90%) confidence level. (The best estimate of β is 1.53, with a 90% range spanning 0.29 to 4.65; the F -test P -value is 0.06.) Less accurate simulation in the early part of the century could be due to problems with observed data, forcing, model response, or simply a result of chance.

[9] The fact that modeled precipitation responds to external (volcanic) forcing was established by Robock and Liu [1994]. Evidence for an effect on observed precipitation has also been reported (e.g., <http://www.giss.nasa.gov/data/precipcru/graphs/>). Quantitative comparison of model and data allows us to assess whether the modeled precipitation signal is of the correct magnitude. Values of β and F and visual inspection of Figure 1 suggest that the model may be underestimating the amplitude of forced response for 1944–97. It may also be underestimating the amplitude of internal precipitation variability, although not by a significant margin, as indicated by the F -test value. Both modelled and observed precipitation signals seem to be dominated by the response to natural forcings, in particular the response to stratospheric aerosols due to volcanic activity as inferred from Figure 1 [see also Sato *et al.*, 1993]. This is in contrast to global land temperature anomalies, which are dominated by the response to anthropogenic forcings [e.g., Stott *et al.*, 2000].

4. Predictability of Precipitation

[10] We can estimate the degree to which precipitation is controlled externally by comparing the variance of the

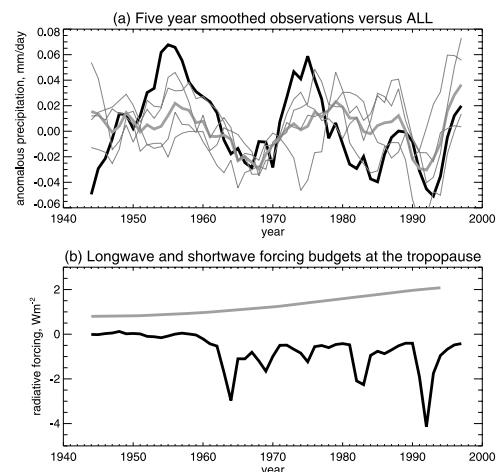


Figure 1. (a) Observed and ALL forcings model-simulated mean time series compared for 1944–97. The thick black line represents observations, the thick grey line the model ensemble mean and the thin grey lines individual ensemble members. All are series of anomalous precipitation and are smoothed with a 5-year boxcar filter. The model series are “masked” to include only the same areas for which there are data in the observations. The model simulation captures some of the form of the observations but is possibly underestimating the response to forcing. (b) Radiative forcing applied to the HadCM3 climate model: net shortwave forcing in black and GHG longwave forcing in grey. Observed precipitation appears to be responding strongly to large changes in shortwave forcing caused by volcanic activity.

forced and unforced model simulations and the observed data on various timescales. We examine variability over 5–10 year periods by subtracting 11-year boxcar filtered annual mean data from 5-year filtered data and 10–20 year variability by subtracting 21-year filtered data from 11-year filtered data.

[11] Potential predictability, pp , is defined as

$$pp = \frac{\text{var}(\text{ens.mean}) - 0.25\text{var}(\text{control})}{(\text{var}(\text{ens.mean}) - 0.25\text{var}(\text{control})) + \text{var}(\text{control})} \quad (1)$$

for a four member ensemble, where $\text{var}(\text{ens.mean})$ is the variance of the forced ensemble mean filtered to extract a specific timescale and $\text{var}(\text{control})$ is the mean variance of identically prepared control segments [e.g., Stott *et al.*, 2000]. pp is the fraction of the variance which can be accounted for by the response of a hypothetical infinite ensemble mean. Assuming that the model control integration provides a realistic simulation of natural variability, it is an upper bound for predictability where the forcings are known and the observations contain no errors. The values derived for 1944–97 land precipitation are 30% for 5–10 year and 45% for 10–20 year variability. For 1908–97, pp is 24% for 5–10 year variability and 35% for 10–20 year variability.

[12] We can also calculate the actual proportion of precipitation changes that are described by forcing on various timescales by correlating appropriately filtered model and observed time series following Stott *et al.*

[2000]. The square of the correlation coefficient is then the normalized covariance of the two series. For the period 1944–97, this covariance is found as 31% for 5–10 year variability and 64% 10–20 year variability (compare with 20% for 5–10 year and 14% for 10–20 year temperature over the same period). The corresponding numbers for the period 1908–97 are 21% for 5–10 year variability and 39% for 10–20 year variability (compare with 6% for 5–10 year and 12% for 10–20 year for temperature). Taken with the values derived for pp , these numbers indicate that we should not expect better agreement between model and observations than these simulations provide. The exception appears to be 10–20 year variability for the period 1944–97, for which the forced simulation agrees with observations more closely than expected, presumably due to chance. We also note that, despite our expectation that precipitation observations should be less predictable than temperature observations, forced variance is describing a larger proportion of observations in the precipitation case on 5–10 and 10–20 year timescales. We believe that this reflects the differing timescales of the forcings which are controlling these two quantities: if we examine greater than 10-year variability for 1908–97, temperature predictability increases to 88% while precipitation predictability falls to zero.

5. Perturbation Energy Balance in the Troposphere

[13] We detect a predictable precipitation response to external forcing which behaves differently to the predictable temperature response investigated by *Stott et al.* [2000]. This might seem surprising as atmospheric moisture content is approximately proportional to global mean temperature [e.g., *Hulme et al.*, 1998]. However, changes in precipitation are accompanied by changes in latent heating of the troposphere, $L\Delta P$, and are necessarily constrained by the conservation of energy [*Mitchell et al.*, 1987; *Allen and Ingram*, 2002; *Yang et al.*, 2003]. To first order,

$$L\Delta P \simeq k_T\Delta T + \Delta R_c + \Delta R_s, \quad (2)$$

where $k_T\Delta T$ describes changes in radiative and sensible cooling due to changes in tropospheric temperature, ΔR_c describes changes in longwave cooling that are due to changes in atmospheric composition and independent of temperature, and ΔR_s contains changes in direct “shortwave cooling” (reduced shortwave heating) that are also independent of temperature (i.e., not due to temperature-dependent cloud feedbacks).

[14] An increase in precipitation can occur if we warm the troposphere because cooling to space and the surface increases with $k_T\Delta T$. To warm the troposphere, we could either increase shortwave input into the climate system by changing the output of the sun or reducing the concentration of stratospheric aerosols, or increase the concentration of tropospheric GHGs absorbing longwave radiation. If incoming shortwave radiation is increased, a small amount is absorbed directly by the troposphere producing a negative ΔR_s . Eventually, warming due to increased absorption of shortwave radiation at the surface will produce a positive $k_T\Delta T$. If the concentration of anthropogenic GHGs is increased, the net longwave radiative cooling to space and

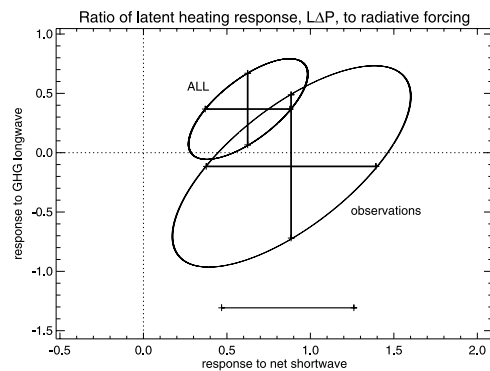


Figure 2. Estimates of the dimensionless ratio $\frac{L\Delta P}{\text{forcing}}$ where changes in latent heat in the observations and ALL ensemble mean are compared with the GHG forcing and net shortwave forcing applied to the model for 1945–93. The ellipses are 2-D 90% confidence limit of the uncertainty for the multiple regression. The lines within the ellipse represent 1-D 90% confidence limits for the amplitude of each forcing with the best estimate of β at the center, the smaller ellipse corresponding to the ensemble mean. The bar at the bottom of the plot represents a 1-D 90% confidence limit for the response to shortwave forcing where the observations are regressed against net shortwave forcing only. The response to shortwave forcing is detected in both observations and model at this level, whereas a response to longwave is not, emphasizing the predominance of shortwave forcing during this period.

the surface produces a negative ΔR_c . For the same ΔT , the ΔR_c produced by an increase in CO_2 is larger than the ΔR_s produced by increasing shortwave input. As a result, a change in anthropogenic GHGs, a longwave forcing, that produces the same change in global mean surface temperature as a shortwave forcing, produces a smaller change in precipitation. This may be the reason we detect a response to external forcing that appears to be dominated by natural shortwave forcings. We note that the correlation between land precipitation and global precipitation in the ALL forcings ensemble of the HadCM3 model is 0.63 during the 20th century. Land-only data, therefore, provide some guide to global changes.

5.1. Response to Specific Forcings

[15] We investigate the response to individual forcings by comparing observations and model to the forcing series; to identify the component of the response which is linear in the forcing. Identically prepared 6-year means of the longwave forcing due to GHGs and net shortwave forcings applied to the model were compared against the observations and the ALL forcings run of the HadCM3 model using an ordinary least squares multiple regression analysis. The influence of shortwave forcing is detected at the 90% level, whereas longwave forcing is not, suggesting again that both the modelled and observed land precipitation responses are dominated by shortwave forcings (Figure 2).

[16] To confirm this explanation, we also analyzed equilibrium HadSM3 slab model experiments forced by CO_2 and changes in solar insolation, both globally and restricted to the land area covered by observed precipitation data (Table 1). The slab model retains the same atmospheric

Table 1. Changes in Temperature, Precipitation and Total Radiative and Sensible Cooling, ΔQ , in HadSM3 Experiments, Showing That the Sensitivity of Precipitation to Changes in Temperature is Highly Dependent on the Nature of the Forcing^a

Run	Forcing, Wm ⁻²	$\frac{\Delta T}{\text{forcing}}$, KW ⁻¹ m ²	$\frac{\Delta P}{\Delta T}$, %K ⁻¹	$\frac{\Delta Q}{\text{forcing}}$	$\frac{L\Delta P}{\text{forcing}}$
2 × CO ₂	3.7	0.93	1.8	1.4	1.4
7.5 Wm ⁻² solar	1.3	0.47	2.8	1.1	1.1
2 × CO ₂ land only	3.7	1.2	1.2	0.50	0.85
7.5 Wm ⁻² solar land only	1.3	0.35	1.5	0.33	0.29

^aThe energy budget is closed globally for both runs, but not for land-only data. Radiative forcing in the solar run was estimated as $\frac{(1-A)S}{4}$ where A represents planetary albedo and S a change in total solar irradiance. Forcing by CO₂ was taken from W. Ingram (personal communication, 2003).

component as HadCM3 but simulates only a single mixed layer thermodynamic ocean.

[17] Total radiative and sensible cooling, ΔQ , balances latent heating, $L\Delta P$, at the global level. The precipitation changes accompanying a given increase in temperature are much smaller than the 6.5% per Kelvin increase predicted by changes in saturation vapor pressure according to the Clausius-Clapeyron equation. The solar forced run exhibits a larger precipitation response per degree of warming than the CO₂ forced run, as expected from the theory outlined earlier in this section, even though the precipitation response per unit forcing is smaller than for CO₂. The relationship breaks down if the data are restricted to land only (see last two rows of Table 1), as equation (1) does not represent all heat fluxes into a restricted portion of the troposphere. However, a larger precipitation response per degree of warming in the solar forced run and a larger precipitation response per unit forcing in the CO₂ forced run remain. We note that the temperature response of HadSM3 to solar forcing is only around 50% of the response to CO₂ forcing. This is outside the usual range of 20% or so reported for the variation in sensitivity to different globally uniform forcings [e.g., Hansen et al., 1997].

6. Conclusion

[18] The influence of known external factors on global land precipitation is detected for the period 1944–97, and more weakly for 1908–97: changes in precipitation are too large to be explained by internal variability alone, and are consistent with the response to combined anthropogenic and natural forcing in a coupled model. Detection experiments using the radiative forcings applied to the model suggest that most of the forced variation is due to shortwave (primarily natural) forcings, as opposed to longwave greenhouse gas (GHG) forcing. However, separate detection of anthropogenic and natural signals in the observations via a multiple regression experiment using HadCM3 model output was unsuccessful.

[19] Energy considerations suggest that a shortwave forcing of the climate system has a larger effect on global precipitation than GHG longwave forcing per degree warming. To the extent that global land precipitation correlates with total precipitation (0.63), the dominance of natural forcing in the 20th century precipitation record could be

explained, even though a GHG longwave forcing is expected to produce a larger response per unit forcing. It also illustrates that a forcing-independent “hydrological sensitivity” is incompatible with energy conservation arguments. Predictions of 21st century hydrology based on sensitivity to 20th century temperature changes are likely to be inaccurate as the ratio of short and longwave forcings may be different in the future.

[20] **Acknowledgments.** We thank Dr Mike Hulme at the Tyndall Centre for Climate Change Research at the University of East Anglia (UEA) for the observed precipitation dataset: ‘gu23wld0098.dat’ (Version 1.0) constructed and supplied at the Climatic Research Unit, UEA, Norwich, UK, with support from the UK Department of the Environment, Transport and the Regions (Contract EPG 1/1/85). We also thank Nathan Gillett and Alan Robock for thorough reviews. FHL was supported by a NERC CASE studentship with CEH Wallingford, PAS by the UK Department for Environment, Food and Rural Affairs under contract PECD 7/12/37.

References

- Allen, M. R., and W. J. Ingram (2002), Constraints on the future changes in climate and the hydrological cycle, *Nature*, *419*, 224–232.
- Allen, M. R., and P. A. Stott (2003), Estimating signal amplitudes in optimal fingerprinting, part I: Theory, *Clim. Dyn.*, *21*, 477–491.
- Gillett, N. P., F. W. Zwiers, A. J. Weaver, and P. A. Stott (2003), Detection of human influence on sea level pressure, *Nature*, *422*, 292–294.
- Gordon, C., C. Cooper, C. A. Senior et al. (2000), The simulation of SST, sea ice extents and ocean heat transports in a version of the Hadley Centre coupled model without flux adjustments, *Clim. Dyn.*, *16*, 147–168.
- Hansen, J., M. Sato, and R. Ruedy (1997), Radiative forcing and climate response, *J. Geophys. Res.*, *102*, 6831–6864.
- Hasselmann, K. (1993), Optimal fingerprints for the detection of time-dependent climate-change, *J. Clim.*, *6*, 1957–1971.
- Hulme, M. (1992), A 1951–80 global land precipitation climatology for the evaluation of General Circulation Models, *Clim. Dyn.*, *7*, 57–72.
- Hulme, M., T. J. Osborn, and T. C. Johns (1998), Precipitation sensitivity to global warming: Comparison of observations with HadCM2 simulations, *Geophys. Res. Lett.*, *25*, 3379–3382.
- Johns, T. C., et al. (2003), Anthropogenic climate change for 1860 to 2100 simulated with the HadCM3 model under updated emissions scenarios, *Clim. Dyn.*, *20*, 583–612.
- Mitchell, J. F. B., C. A. Wilson, and W. M. Cunningham (1987), On CO₂ climate sensitivity and model dependence of results, *Q. J. R. Meteorol. Soc.*, *113*, 293–322.
- New, M., M. Hulme, and P. Jones (2000), Representing twentieth-century space-time climate variability. Part II: Development of 1901–96 monthly grids of terrestrial surface climate, *J. Clim.*, *13*, 2217–2238.
- Robock, A., and Y. Liu (1994), The volcanic signal in Goddard Institute for Space Studies three-dimensional model simulations, *J. Clim.*, *7*, 44–55.
- Sato, M., J. E. Hansen, M. P. McCormick, and J. B. Pollack (1993), Stratospheric aerosol optical depths, 1850–1990, *J. Geophys. Res.*, *98*, 22,987–22,994.
- Spencer, R. W. (1993), Global oceanic precipitation from the MSU during 1979–91 and comparison to other climatologies, *J. Clim.*, *6*, 1301–1326.
- Stott, P. A., S. F. B. Tett, G. S. Jones et al. (2000), External control of 20th century temperature by natural and anthropogenic forcings, *Science*, *290*, 2133–2137.
- Tett, S. F. B., et al. (2002), Estimation of natural and anthropogenic contributions to twentieth century temperature change, *J. Geophys. Res.*, *107*(D16), 4306, doi:10.1029/2000JD000028.
- Yang, F., A. Kumar, M. E. Schlesinger, and W. Wang (2003), Intensity of hydrological cycles in warmer climates, *J. Clim.*, *16*, 2419–2423.

M. R. Allen and F. H. Lambert, Atmospheric, Oceanic and Planetary Physics, Clarendon Laboratory, Parks Road, Oxford, OX1 3PU, UK. (hlambert@atm.ox.ac.uk)

M. A. Palmer, Space Science and Technology Department, Rutherford Appleton Laboratory, Didcot, Oxfordshire, OX11 0QX, UK.

P. A. Stott, Met Office, University of Reading, Reading, RG6 6BB, UK.